Carbohydrate Polymers 220 (2019) 157–162

Contents lists available at ScienceDirect

Carbohydrate Polymers

journal homepage: www.elsevier.com/locate/carbpol

Molecular partitioning in ternary solutions of cellulose

Xin Zhang[a], Yimin Mao[a,b], Madhusudan Tyagi[a,b], Feng Jiang[a], Doug Henderson[a], Bo Jiang[a], Zhiwei Lin[a], Ronald L. Jones[c], Liangbing Hu[a], Robert M. Briber[a], Howard Wang[a,c,*]

[a] Department of Materials Science and Engineering, University of Maryland, College Park, MD, 20742, United States
[b] NIST Center for Neutron Research, National Institute of Standards and Technology, Gaithersburg, MD, 20899, United States
[c] Material Measurement Laboratory, National Institute of Standards and Technology, Gaithersburg, MD, 20899, United States

ARTICLE INFO

Keywords:
Cellulose
Ionic liquid
Neutron scattering
Molecular solution
Phase diagram

ABSTRACT

Neutron scattering measurements on the structure and dynamics of ternary solutions of microcrystalline cellulose (MC) in mixtures of an ionic liquid (IL) 1-ethyl-3-methylimidazolium acetate and a polar organic solvent dimethylformamide (DMF) have shown that MC can be fully dissolved in solvent mixtures. Data also show the molecular partitioning of IL into coexisting states. The structure partitioning is manifested as IL adsorbed to cellulose molecules with additional IL self-assembled to form clusters in solution, while the dynamics partitioning shows dynamical heterogeneities of the IL with slow dynamics resembling neat IL and fast dynamics being coupled with the solvent. The composition dependence of the molecular partitioning results in a solubility gap in dilute cellulose solutions and a phase boundary criterion of the molar ratio of IL / MC ~ 3 in more concentrated regimes. The two characteristics together define the main features of the dissolution phase diagram of ternary cellulose mixtures of MC / IL / DMF at the room temperature.

1. Introduction

Cellulose is attractive for its chemical, mechanical and biological properties; it is the most abundant polymer on earth, and a suitable material for sustainable manufacturing. Cellulose in its natural crystalline form is insoluble in water and most organic solvents, in part due to co-existing hydrophilic and hydrophobic interactions between the anhydroglucose units (AGU) (Klemm, Heublein, Fink, & Bohn, 2005; Medronho & Lindman, 2015; Moon, Martini, Nairn, Simonsen, & Youngblood, 2011) along the backbone. In manufacturing cellulosic products involving molecular-level engineering, harsh chemical processes have been employed (Klemm et al., 2005) to separate cellulose chains from crystalline fibers, dissolve into solution, process, and regenerate to form useful compositions and structures for particular applications. Alternative methods using environmentally friendly processes and chemicals have been actively pursued in recent decades, (Potthast et al., 2002; Wachsmann & Diamantoglou, 1997; Wang, Gurau, & Rogers, 2012; Zhang, Ruan, & Gao, 2002; Zhang, Ruan, & Zhou, 2001) among which using ionic liquids shows the promise of efficacy and greenness (Hayes, Warr, & Atkin, 2015; Holding et al., 2017; Swatloski, Spear, Holbrey, & Rogers, 2002; Wang et al., 2012). In practice, aprotic polar solvents are often added to minimize the amount of IL, reduce the viscosity, accelerate the dissolution process, retain contaminants, and reduce cost. While the application of ILs in dissolving cellulosic materials has been recognized since the early 20th century (Graenacher, 1934), fundamental knowledge of molecular interactions and mesoscopic structures in some common ternary mixtures of cellulose, IL and solvents remains limited.

The local and atomic coordination of ILs with cellulose and solvents has been investigated using nuclear magnetic resonance (NMR) spectroscopy (Remsing, Swatloski, Rogers, & Moyna, 2006; Zhang et al., 2010), highlighting the role of competing hydrogen-bond formation in the solvation process. While chemical structure and functional group interactions and their effect on cellulose dissolution have been the focus of extensive research, probes at atomic and chemical bond levels do not reveal the structure and dynamics at length scales over which molecular partitioning may occur. In fact, partitioning of molecules in mixtures to form mesoscopic scale structures, such as preferential association of ILs with cellulose or self-assembly, play a significant role on properties relevant to solution processing such as solubility, rheology, diffusion and regeneration. Meso-structures in cellulose solutions generally fall in the measurement range of small angle scattering. Previous studies on cellulose dissolution in IL and organic solvent mixtures using small angle neutron scattering (SANS) have shown that IL/dimethylformamide (DMF) mixture is a good solvent for cellulose while IL/dimethylsulfoxide (DMSO) is a θ-solvent. (Napso, Rein, Khalfin, & Cohen,

* Corresponding author at: Department of Materials Science and Engineering, University of Maryland, College Park, MD, 20742, United States.
E-mail address: wangh@umd.edu (H. Wang).

https://doi.org/10.1016/j.carbpol.2019.05.054
Received 20 February 2019; Received in revised form 9 May 2019; Accepted 17 May 2019
Available online 23 May 2019
0144-8617/

2017; Rein, Khalfin, Szekely, & Cohen, 2014)

Several groups have reported cellulose/IL/solvent phase diagrams, particularly with DMSO as a co-solvent (Holding et al., 2017; Le, Rudaz, & Budtova, 2014), this study focuses on the ternary mixtures of cellulose with the IL of 1-ethyl-3-methylimidazolium acetate (EMIMAc) and DMF co-solvent to understand the dissolution parameter space and the partitioning behavior of EMIMAc in solution. EMIMAc was used in this study because it dissolves cellulose well, has a low viscosity, and is halogen free. The goal of this study is to more precisely map the dissolution phase boundaries of the ternary cellulose system containing EMIMAc and DMF, and further elucidate the molecular behavior of cellulose and IL using a combination of light and neutron scattering techniques. We have shown that the ternary mixtures have different behavior with the DMF as co-solvent compared to those with DMSO, particularly near the vicinity of the neat solvent.

2. Experiment

The microcrystalline cellulose (Avicel PH101, MC) and the ionic liquid EMIMAc were purchased from Sigma-Aldrich,[1] and per deuterated DMF (dDMF) was purchased from Cambridge Isotope.[1] Cellulose and IL were dried in vacuum at 60 °C overnight and stored in a dry glovebox. Deuterated DMF arrived in ampoules and was used without further purification. Non-deuterated DMF was reagent grade and dried with molecular sieves. Avicel PH101 is purified cellulose with the degree of polymerization of the average number of AGU per cellulose chain, DP ≈ 250, as provided by the supplier.[1] As all three components are hygroscopic, ternary mixtures were prepared in a dry glovebox to minimize the water absorption.

EMIMAc has a nominal purity of ≥ 95% by mass as specified by the supplier. The water content is less than 1% by mass as measured using a Bruker Avance 400 NMR. The volatile content in EMIMAc is *ca.* 2% by mass up to a temperature of 413 K as measured using a TA SDT650 thermogravimetric analysis (TGA). The electric conductivity of EMIMAc / DMF solutions was measured using a BioLogic VMP3 potentiostat at the room temperature. More measurement details are included in the supporting materials.

Cellulose and DMF were premixed and left settle in sealed vials overnight. The cellulose / DMF mixtures were preheated to 363 K, and then IL was gradually injected to mixtures under mechanical agitation through a silicone septum in the cap without opening the vial. For low concentration mixtures, clear solutions are achieved immediately after the addition of IL. Vials containing mixtures were placed in a sand bath at 363 K for homogenization. The sand bath heated up the mixtures rapidly, typically achieving dissolution within a minute. Higher viscosity solutions required longer times for homogenization. In the soluble regime, a clear solution could be typically obtained in a few minutes. If a mixture did not become clear after 1 h at 363 K, the mixture is marked red as an insoluble composition. After achieving clear solutions at 363 K, the mixtures were held at room temperature for 24 h. If any cloudiness or aggregates were discernible by eye or using an Olympus BX60 F cross-polarized microscope, it is marked as orange in the ternary diagram map; if the solution remains clear, it is further characterized using SANS.

SANS measurements were carried out at the NIST Center for Neutron Research (NCNR) at the National Institute of Science and Technology (NIST), Gaithersburg, Maryland. Typical SANS spectra were obtained with a neutron wavelength, $\lambda \approx 6$ Å, and a wavelength spread $\Delta\lambda/\lambda \approx 0.12$. Three instrumental configurations, with sample-to-detector distances of 13 m, 4 m and 1 m, respectively, were used to collect scattering data covering a Q -range between 0.003 $Å^{-1}$ to *ca.* 0.5 $Å^{-1}$ (the scattering momentum transfer vector; $Q = \left(\frac{4\pi}{\lambda}\right)\sin\theta$, with θ being half of the scattering angle). Data reduction were carried out using the IGOR Pro macros (available from NCNR), (Kline, 2006) which involves subtracting background signal from the environment and the empty cell, correcting for detector efficiency, converting to absolute scattering cross-section, and averaging 2D data into 1D spectra, *I(Q)*, which is the density of the total scattering cross-section for all the molecules of cellulose, EMIMAc and DMF in the scattering volume.

The local dynamics of selected specimens, including neat IL, organic solvent, a binary mixture of IL and solvent, and a ternary mixture, have been measured using the High Flux Backscattering Spectrometer (HFBS) at the NCNR. In a typical experiment, HFBS was operated in Doppler stopped mode. All samples were cooled from 294 K to 4 K, and elastic intensities were recorded in the Q range of 0.25 $Å^{-1}$ – 1.75 $Å^{-1}$. Such measured elastic intensity can be used to calculate mean square displacement (MSD) using standard Gaussian approximation, $\frac{I(T)}{I_0} = exp\left(-\frac{Q^2 < u^2(T) >}{3}\right)$, where *I(T)* and I_0 are the elastic intensity at a given temperature, T, and at the lowest measured temperature of 4 K, where signal is expected to be purely elastic, respectively. $< u^2(T) >$ is the average MSD of the dominant scattering atoms in the specimen.

3. Results

The ternary cloud point phase diagram at ambient temperature, $T = 293$ K, is shown in Fig. 1(a), while the solvent corner of the phase diagram shown in Fig. 1(b). To simplify the notion of ternary compositions, coordinate notions based on the molar percentage values of cellulose (C), ionic liquid (I), and solvent (S) are used, in which C is calculated based on moles of AGU, and I and S by moles of molecules, respectively. For example, in Fig. 1(b), the upper corner C0 I20 S80 represents 20 mol% IL and 80 mol% DMF without the cellulose, and the lower left corner C0 I20 S80 is 20 mol% AGU and 80 mol% DMF without IL. Three types of behaviors were observed by combining optical cloud point and SANS measurements: (1) clear at 293 K, green symbols; (2) clear at 363 K but cloudy at 293 K, orange symbols; and (3) cloudy at both 293 K and 363 K, red symbols. The solid curves are visual guides to divide the diagram into the upper one-phase and the lower aggregation regimes, and the dashed line in Fig. 1(b) is the asymptote I / C = 3.

While there is room for improvement as to the exact location of the phase boundaries in the composition map, certain features of the phase diagram are non-ambiguous. In compositional regimes where DMF is not the dominant majority, *i.e.*, greater than 85 mol%, the dissolution boundary approximately follows the line at I / C = 3 ratio. However, this simple ratio rule breaks down around the intersection of I / C = 3 and I15 lines, below which higher I / C ratio is required to achieve stable clear solutions of cellulose. The critical I / C dissolution ratio diverges at roughly C0 I5 S95, *i.e.*, the solubility of cellulose in 5 mol% IL goes to zero at room temperature. There exists a solubility gap near the DMF-rich corner of the phase diagram, implying different dissolution behaviors comparing to the ternary system of cellulose, EMIMAc and DMSO (Le et al., 2014).

SANS spectra of ternary mixtures of 0.3 mol% and 1 mol% cellulose in IL/DMF, and a binary ionic solution of C0 I10 S90, are shown in Fig. 2. SANS of the IL solution C0 I10 S90 (solution 5) exhibits a notable fall off in scattering at high Q, implying a dilute solution of uniform particulates. Fitting the spectrum using the Guinier law for an isolated particulate dispersion yields the average radius of gyration, $R_g = 0.76$ nm, corresponding to EMIMAc clusters each in average consisting of *ca.* 15 molecules. Electric conductivity measurements on a series of EMIMAc / DMF solutions with varying concentrations reveal a critical aggregation concentration (CAC) at *ca.* 2 mol%, as shown in the supplementary materials.

Both C0.3 I4.8 S94.9 (solution 4) and C1 I9.5 C89.5 (solution 3) are

[1] Disclaimer: The identification of any commercial product or trade name does not imply endorsement or recommendation by the National Institute of Standards and Technology.

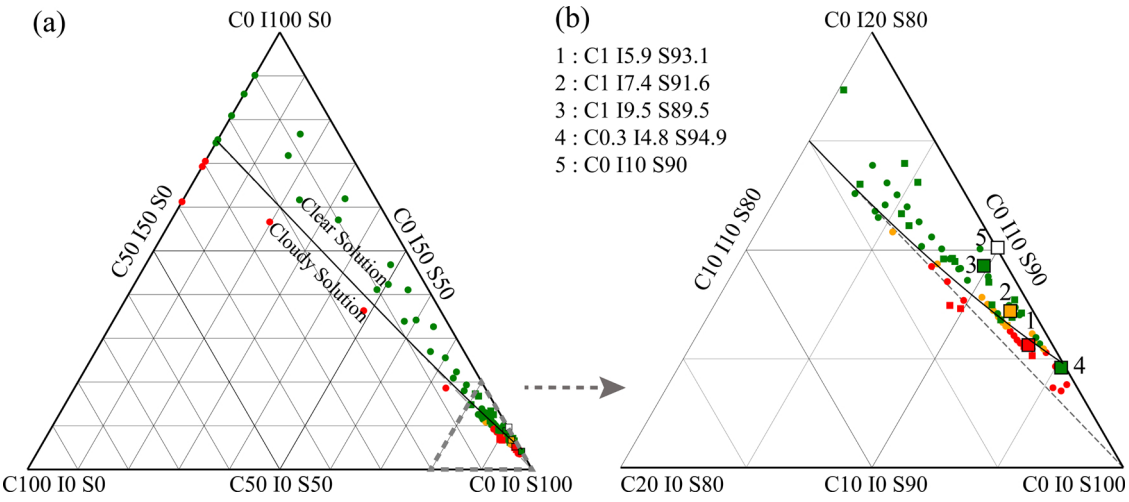

Fig. 1. (a), Cellulose (C), ionic liquid EMIMAc (I) and organic solvent DMF (S) cloud point phase diagram. Circular markers are data from using non-deuterated DMF and square markers per deuterated DMF. Symbol labels are as follows: clear at 293 K, green; clear at 363 K but cloudy at 293 K, orange; and cloudy at both 293 K and 363 K, red. The solid curves divide the diagram to the upper one-phase regime and the lower aggregation regime. (b) Detailed phase diagram near the solvent rich corner. Compositions labeled 1 to 5 are compositions corresponding to SANS data labeled 1 to 5 in Fig. 2. The dashed line is the asymptote of I / C = 3 M ratio (For interpretation of the references to colour in this figure legend, the reader is referred to the web version of this article).

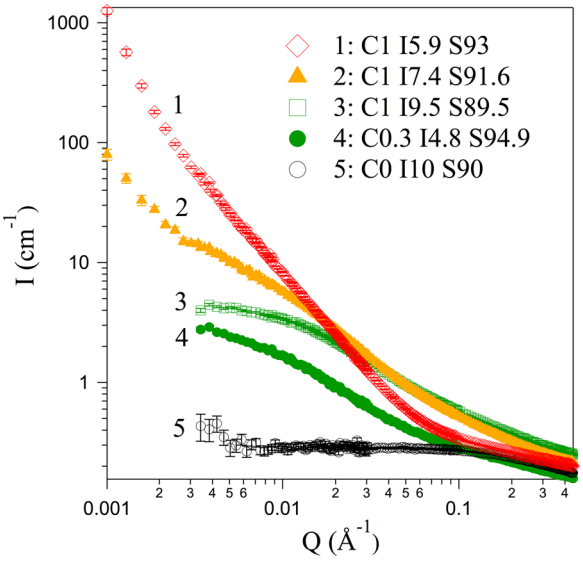

Fig. 2. Typical SANS spectra of ternary mixtures. C0 I10 S90 the IL solution shows uniform clusters of *ca.* 1 nm. C0.3 I4.8 S94.9 and C1 I9.5 C89.5 are clear cellulose solutions of molecular coils. C1 I7.4 S91.6 and C1 I5.9 S93 are solutions with aggregates. The number labels of SANS spectra in the figure correspond to the composition label in Fig. 1(b).

uniform stable cellulose solutions with no aggregates or precipitates, they are marked in the phase diagram map in Fig. 1(b) as green squares with the corresponding number labels. For both solutions, SANS data at low *Q* has a relatively low intensity and approaches an asymptote, implying homogeneous dissolution at the molecular level. Molecular solution of cellulose in EMIMAc / DMF has been reported and the mechanism been attributed to direct absorbing of EMIMAc onto cellulose (Rein et al., 2014; Raghuwanshi et al., 2018). The solutions C0.3 I4.8 S94.9 and C1 I9.5 C89.5 fall to the dilute and semi-dilute regimes of coil solutions, respectively, consistent with the findings in the previous report. (Rein et al., 2014)

For both C1 I7.4 S91.6 (solution 2) and C1 I5.9 S93 (solution 1) the rapid upturn of the scattering intensity in the low-*Q* range implies the formation of aggregates on length scales of a hundred nanometers or larger. However, the two solutions are different, cellulose aggregation could not be eliminated at 363 K for I / C = 5.9 (solution 1); reversible clustering occurs for I / C = 7.4 (solution 2) as the gel turned into a clear viscous solution by heating to 363 K.

To quantitatively assess the partitioning of IL in ternary solutions, SANS has been carried out on a series of specimens with increasing cellulose concentration at a fixed co-solvent molar ratio of I / S = 15 / 85. Fig. 3 shows SANS of the series with cellulose concentrations up to 2.77 mol%, in which the symbols are experimental data and the curves through symbols are the best model fitting. The model is a superposition of a power law to capture the low-*Q* excess scattering, a Lorentz function to describe cellulose coil correlations in the mid-*Q* region, and a Guinier law at high-*Q*, yielding a nm-scale correlation length of overlapping coils, l, and R_g of nano-clusters, respectively. Quantities

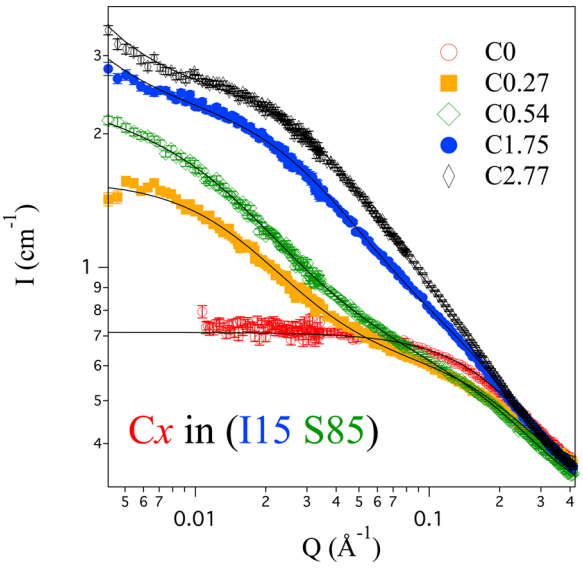

Fig. 3. SANS spectra of a series of cellulose solutions with fixed I / S = 15 / 85 ratio and increasing C fractions. The symbols are experimental data and the curves through symbols are the best model fitting, which is a superposition of a power law to capture the low-*Q* excess scattering, a Lorentzian function to describe the composition correlation at the mid-Q, and a Guinier law at high-*Q*. Data reveal scattering from molecular cellulose, clusters of IL assembly in solvents, and the adsorption of IL on cellulose as C increases.

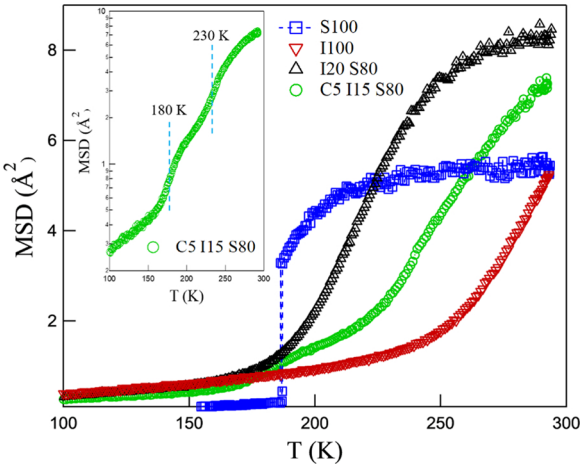

Fig. 4. Mean square displacement (MSD) of the neat solvent dDMF (S100), neat IL (I100), the IL/dDMF mixture (I20 S80), and the MC/IL/DMF solution (C5 I15 S80) as measured using neutron backscattering during cooling scan from 293 K to 4 K (only data above 100 K are shown for clarity). The cellulose solution displays two distinct dynamics transitions, at around 230 K and 180 K, respectively, as shown in the inset in semi-logarithm scales.

obtained from model fitting are listed in the supplementary materials. The main findings are summarized as follows.

In dilute solutions C0.27 and C0.54, in addition to the characteristic IL cluster scattering as observed in C0, the low-Q plateau implies molecular dissolution of the cellulose in the I15 S85 solvent mixture, with a correlation length $l \approx 6$ nm from the model fitting. A suppression of the intensity of the cluster scattering indicates a reduced IL cluster concentration due to IL adsorption to the cellulose. With $R_g \approx 0.76$ nm for the IL clusters, the average adsorption ratio of EMIMAc to AGU in dilute solutions of cellulose with the excess IL, has been estimated to be I / C ≈ 10 (data and calculation in the supplementary material). As the concentration of cellulose increases, at C2.77, l decreases to *ca.* 2 nm, implying a smaller mesh dimension in more concentrated cellulose solutions.

The mean square displacement (MSD) averaged over all species as measured by quasielastic neutron scattering as a function of temperature is shown in Fig. 4. The samples include neat dDMF (S100), neat IL (I100), IL in dDMF (I20 S80), and a ternary mixture of cellulose, IL and dDMF (C5 I15 S80). Except for S100, the MSD reflects mostly the mobility of IL in the sample since large scattering cross-section of hydrogen dominates the signal compared to other elements in the system, which is obvious in I100 and I20 S80 and also true in C5 I15 S80, in which the number of IL hydrogen atoms is 4 times that of cellulose. The I100 shows vitrification over a wide temperature range, with most mobility loss on cooling having occurred by 230 K; whereas S100 shows a sharp transition at 190 K, corresponding to the freezing of dDMF. The solvent mixture I20 S80 loses mobility as a function of temperature from far above to below the dDMF crystallization, implying strong interactions between IL and dDMF. The cellulose solution C5 I15 S80 shows very different features, displaying two distinct dynamic transitions. An expanded plot of the two dynamic arresting processes upon cooling is shown in the inset of Fig. 4 as semi-logarithm plot, in which two transitions are marked at around 230 K and 180 K, respectively.

4. Discussion

The dissolution phase boundary feature of I / C = 3 in Fig. 1 is consistent with a stoichiometric ratio of one IL molecule for each of the three hydroxyl (OH) hydrogen bonding sites on one AGU. The binding of the EMIMAc molecules on cellulose has been studied using NMR (Remsing et al., 2006; Zhang et al., 2010), indicating the molar ratio of IL / OH between 0.75 and 1 in the primary solvation shell. The data apparently point to a simple dissolution criterion of one-to-one matching of functional groups. However, this simple rule does not apply to solutions with low IL concentrations; there exists a critical IL concentration below which cellulose is not soluble at all. The existence of a dissolution gap near the DMF-rich corner of the phase diagram is a strong indication of molecular partitioning of IL and the formation of clusters. IL molecules exist in three forms in ternary solutions: isolated individual molecules, aggregated in clusters, or absorbed as a solvation shell on cellulose chains. They exchange among cluster and cellulose solvation layers through individual IL molecules in solvent, reaching a dynamic equilibrium. The critical cluster concentration is at *ca.* 2 mol %; in a typical ternary solution with ionic liquid concentration greater than 3 mol%, majority of IL are partitioned into clusters and solvation shells in equilibrium.

Molecular partitioning of the IL is also manifested in the dynamics. The measured MSD of I20 S80 and C5 I15 S80 shows that the presence of cellulose in solvent mixture decreases the MSD of IL, indicating smaller overall mobility of IL in cellulose solution, which is consistent with the SANS data that imply the association of the IL with the cellulose. Further, the dynamic heterogeneity with two distinct dynamic transitions implies that at least two species of IL, slow and fast, exist in the ternary mixtures which is also consistent with the two species of IL revealed in SANS, *i.e.*, those in solvation shells and those as individual molecules or clusters in solvent, respectively. The arrest in the slow dynamics at higher temperatures is attributed to IL strongly associated with cellulose, whereas the fast species are the IL as individual molecules and clusters in the organic solvent. The imidazole group in EMIMAc is a weaker donor of hydrogen bonding than the hydroxyl groups on cellulose (Remsing et al., 2006; Zhang et al., 2010), however, the combination of hydrophilic and hydrophobic interactions, and possibly favorable stereochemical interactions facilitate strong bonding of EMIMAc to the rigid and long chain molecules of cellulose, resulting in the slow dynamics. The data imply the partitioning of IL molecules in two dynamic species, those tightly-bound to cellulose having slow dynamics, and those in solvent mixtures or loosely associated with cellulose having fast dynamics.

A phenomenological model of cellulose dissolution in ionic liquid and organic solvent mixtures emerges from the dissolution phase diagram and neutron scattering, as schematically illustrated in Fig. 5. At high cellulose concentrations, the availability of high energy binding sites facilitates IL molecules associating with cellulose chains to form a solvation shell, resulting in a network of solvated cellulose chains, as depicted schematically in Fig. 5(a). Most IL molecules are associated with the cellulose chains, with few IL spherical clusters. At low cellulose concentrations (*e.g.*, 0.54 mol% cellulose in I15 S85 mixtures), relatively extensive cluster formation occurs in solvents; in addition to IL directly binding on cellulose chains to form the first solvation shell, excess IL form an outer second shell, as depicted in Fig. 5(b), resulting in solvated complexes of IL and cellulose chains with molar ration I / C ≈ 10 (shown in supporting materials).

The structure of cellulose solvation resembles that in urea/NaOH aqueous solutions (L. N. Zhang et al., 2002; Zhang et al., 2001), in which IL molecules bind with cellulose chains to form complexes that are soluble in DMF, just like urea/NaOH bind with cellulose to form complexes that are soluble in water. Favorable specific interactions between IL and cellulose dominate at high cellulose concentrations, and solvated chains stabilize in the solvent with a finite mesh size as characterized by the correlation length from SANS. The tendency toward forming spherical clusters in dilute cellulose solutions is driven by the interplay between the enthalpy of self-limiting ionic aggregations and the entropy associated with the spatial volume for accommodating isolated spherical clusters. The latter is mostly responsible for the existence of the solubility gap at the low IL concentration near the solvent-rich corner. The dissolution of cellulose is a result of competitive partitioning of IL molecules between solvated chains and clusters. In the

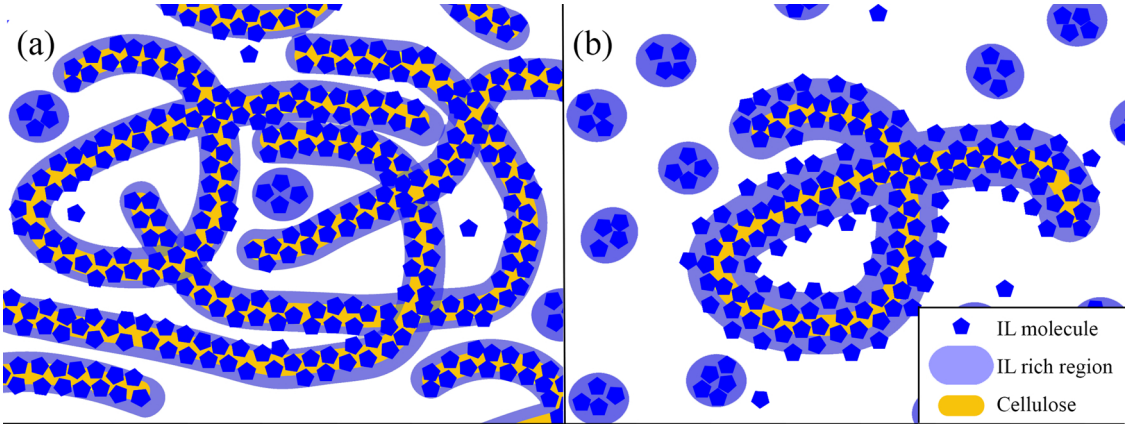

Fig. 5. Schematic illustration of the cellulose dissolution using ionic liquid in organic solvents. (a) At high cellulose concentration, IL tightly-bond to cellulose chains to form a thin shell, resulting in a network of worm-like micelles. As most IL bonded to cellulose, few clusters form due to limited free ILs. (b) At low cellulose concentrations, the IL shell is made of the tight-binding ILs directly on cellulose and loose outskirt layers, and clusters form relatively extensively in solvents.

dilute limit of both the cellulose and IL, the larger accessible space is the favorable entropic driving force of cluster formation, tilting the partitioning of IL from solvation shells toward clusters, resulting in diminished solubility of cellulose and a dissolution gap.

The structural partitioning of IL has dynamic consequences, causing dynamics partitioning of ILs: those directly associated with cellulose would be the slow dynamics species resembling those in solvent have fast dynamics. It is noted that the structural and dynamic partitioning may not strictly coincide with each other, as the IL in the outer solvation shell is rather mobile and in dynamic equilibrium with ILs in solvent. A better understanding of molecular partitioning and mesoscopic structure forming will help develop cellulose technologies from a molecular perspective.

5. Summary

In summary, the molecular level study on ternary mixtures of cellulose, ionic liquids, and polar organic solvent DMF have revealed dissolved cellulose molecular coils and the bimodal partitioning of IL affecting both structure and dynamics. The structural partitioning manifests as ILs adsorbed to cellulose (tightly or loosely) and IL aggregated into clusters dispersed in the aprotic solvent, while dynamic partitioning distinguishes two dynamic species: slow dynamics of IL strongly bonded to cellulose and fast dynamics of IL in solution as well as on outer cellulose solvation shells in rapid exchange with those in solution. The states of molecular partitioning in structure and dynamics determine the dissolution phase diagram of the ternary system. At high cellulose concentrations, the solubility boundary approximately follows $I / C \approx 3$, while in the dilute limit, a solubility gap for cellulose exists at the vicinity between co-solvent line of *ca.* I5 S95 and S100, in which the dissolution power of the IL-solvent mixtures for cellulose diminishes. The balance between the entropy of spherical IL clusters in solvent and the exchange enthalpy of IL in clusters and solvation shells of cellulose plays an essential role.

Acknowledgements

HW acknowledges the financial support of NIST Award 70NANB12H238, and the use of the cold neutron facility at the NIST Center for Neutron Research. Portions of this work benefited from and provided support to the NIST nSoft consortium (www.nist.gov/nsoft), including use of the 10-meter Small Angle Neutron Scattering instrument at the NCNR. Access to NGB 30 m SANS and the HFBS beamlines at the NIST Center for Neutron Research was provided by the Center for High Resolution Neutron Scattering, a partnership between the National Institute of Standards and Technology and the National Science Foundation under Agreement No. DMR-1508249

Appendix A. Supplementary data

Supplementary material related to this article can be found, in the online version, at doi:https://doi.org/10.1016/j.carbpol.2019.05.054.

References

Graenacher, C. Cellulose solution, U.S. Patent 1,943,176, 1934.
Hayes, R., Warr, G. G., & Atkin, R. (2015). Structure and nanostructure in ionic liquids. *Chemical Reviews, 115*(13), 6357–6426. https://doi.org/10.1021/cr500411q.
Holding, A. J., Parviainen, A., Kilpelainen, I., Soto, A., King, A. W. T., & Rodriguez, H. (2017). Efficiency of hydrophobic phosphonium ionic liquids and DMSO as recyclable cellulose dissolution and regeneration media. *RSC Advances, 7*(28), 17451–17461. https://doi.org/10.1039/c7ra01662j.
Klemm, D., Heublein, B., Fink, H. P., & Bohn, A. (2005). Cellulose: Fascinating biopolymer and sustainable raw material. *Angewandte Chemie-International Edition, 44*(22), 3358–3393. https://doi.org/10.1002/anie.200460587.
Kline, S. R. (2006). Reduction and analysis of SANS and USANS data using IGOR Pro. *Journal of Applied Crystallography, 39*, 895–900. https://doi.org/10.1107/s0021889806035059.
Le, K. A., Rudaz, C., & Budtova, T. (2014). Phase diagram, solubility limit and hydrodynamic properties of cellulose in binary solvents with ionic liquid. *Carbohydrate Polymers, 105*, 237–243. https://doi.org/10.1016/j.carbpol.2014.01.085.
Medronho, B., & Lindman, B. (2015). Brief overview on cellulose dissolution/regeneration interactions and mechanisms. *Advances in Colloid and Interface Science, 222*, 502–508. https://doi.org/10.1016/j.cis.2014.05.004.
Moon, R. J., Martini, A., Nairn, J., Simonsen, J., & Youngblood, J. (2011). Cellulose nanomaterials review: Structure, properties and nanocomposites. *Chemical Society Reviews, 40*(7), 3941–3994. https://doi.org/10.1039/c0cs00108b.
Napso, S., Rein, D. M., Khalfin, R., & Cohen, Y. (2017). Semidilute solution structure of cellulose in an ionic liquid and its mixture with a polar organic co-solvent studied by small-angle x-ray scattering. *Journal of Polymer Science Part B-Polymer Physics, 55*(11), 888–894. https://doi.org/10.1002/polb.24337.
Potthast, A., Rosenau, T., Buchner, R., Roder, T., Ebner, G., Bruglachner, H., ... Kosma, P. (2002). The cellulose solvent system N,N-dimethylacetamide/lithium chloride revisited: The effect of water on physicochemical properties and chemical stability. *Cellulose, 9*(1), 41–53. https://doi.org/10.1023/a:1015811712657.
Raghuwanshi, V. S., Cohen, Y., Garnier, G., Garvey, C. J., Russell, R. A., Darwish, T., & Garnier, G. (2018). Cellulose dissolution in ionic liquid: Ion binding revealed by neutron scattering. *Macromolecules, 51*(19), 7649–7655. https://doi.org/10.1021/acs.macromol.8b01425.
Rein, D. M., Khalfin, R., Szekely, N., & Cohen, Y. (2014). True molecular solutions of natural cellulose in the binary ionic liquid-containing solvent mixtures. *Carbohydrate Polymers, 112*, 125–133. https://doi.org/10.1016/j.carbpol.2014.05.059.
Remsing, R. C., Swatloski, R. P., Rogers, R. D., & Moyna, G. (2006). Mechanism of cellulose dissolution in the ionic liquid 1-n-butyl-3-methylimidazolium chloride: A C-13 and Cl-35/37 NMR relaxation study on model systems. *Chemical Communications,* (12), 1271–1273. https://doi.org/10.1039/b600586c.
Swatloski, R. P., Spear, S. K., Holbrey, J. D., & Rogers, R. D. (2002). Dissolution of cellose with ionic liquids. *Journal of the American Chemical Society, 124*(18), 4974–4975. https://doi.org/10.1021/ja025790m.
Wachsmann, U., & Diamantoglou, M. (1997). Potential of the NMMO-process for the

production of fibres and membranes. *Papier, 51*(12), 660–665.
Wang, H., Gurau, G., & Rogers, R. D. (2012). Ionic liquid processing of cellulose. *Chemical Society Reviews, 41*(4), 1519–1537. https://doi.org/10.1039/c2cs15311d.
Zhang, J., Zhang, H., Wu, J., Zhang, J., He, J., & Xiang, J. (2010). NMR spectroscopic studies of cellobiose solvation in EmimAc aimed to understand the dissolution mechanism of cellulose in ionic liquids. *Physical Chemistry Chemical Physics, 12*(8), 1941–1947. https://doi.org/10.1039/b920446f.
Zhang, L. N., Ruan, D., & Gao, S. J. (2002). Dissolution and regeneration of cellulose in NaOH/thiourea aqueous solution. *Journal of Polymer Science Part B-Polymer Physics, 40*(14), 1521–1529. https://doi.org/10.1002/polb.10215.
Zhang, L. N., Ruan, D., & Zhou, J. P. (2001). Structure and properties of regenerated cellulose films prepared from cotton linters in NaOH/Urea aqueous solution. *Industrial & Engineering Chemistry Research, 40*(25), 5923–5928. https://doi.org/10.1021/ie0010417.